A SIMPLE MODEL-BASED MAGNET SORTING ALGORITHM FOR PLANAR HYBRID UNDULATORS*

G. Rakowsky#, BNL, Upton, NY 11973, U.S.A.

Abstract

Various magnet sorting strategies have been used to optimize undulator performance, ranging from intuitive pairing of high- and low-strength magnets, to full 3D FEM simulation with 3-axis Helmholtz coil magnet data. In the extreme, swapping magnets in a full field model to minimize trajectory wander and rms phase error can be time consuming. This paper presents a simpler approach, extending the field error signature concept to obtain trajectory displacement, kick angle and phase error signatures for each component of magnetization error from a Radia [1] model of a short hybrid-PM undulator. We demonstrate that steering errors and phase errors are essentially decoupled and scalable from measured X, Y and Z components of magnetization. Then, for any given sequence of magnets, rms trajectory and phase errors are obtained from simple cumulative sums of the scaled displacements and phase errors. The cost function (a weighted sum of these errors) is then minimized by swapping magnets, using one's favorite optimization algorithm. This approach was applied recently at NSLS to a short in-vacuum undulator, which required no subsequent trajectory or phase shimming. Trajectory and phase signatures are also obtained for some mechanical errors, to guide "virtual shimming" and specifying mechanical tolerances. Some simple inhomogeneities are modeled to assess their error contributions.

INTRODUCTION

NSLS-II will have numerous planar in-vacuum hybrid-PM undulators (IVU's), designed to deliver high-brightness multi-kilovolt photon beams. They will have period lengths typically on the order of 20 mm and will be optimized for high brightness at high harmonics. This requires minimizing the deleterious effects of field errors, which cause not only deviations in trajectory straightness, but also introduce phase errors which reduce peak brightness, especially at high harmonics. Strategies for minimizing these errors include imposition of tight dimensional tolerances on poles, magnets, module parts and support beams, on tolerance stack-ups, and on precise mounting of these components. The second is requiring tight magnetic tolerances on the permanent magnet (PM) blocks. Magnet manufacturers now routinely achieve magnet strength errors of <1% and magnetization angle errors of <1°. Still, it is routine practice to measure the X, Y and Z magnetic moments of PM's with Helmholtz coils, and to apply some kind of sorting algorithm to minimize undulator field errors and their consequences. Characterizing magnet blocks in a Helmholtz coil or by far field measurements yields the average magnetic moments over the magnet. Magnetic inhomogeneities in the small IVU magnets are inherently small and will be ignored here.

Magnet sorting methods and criteria for optimizing undulators range from intuitive pairing of stronger and weaker magnets to minimize field errors (used as recently as 2007[2]), to multi-parameter optimization by Simulated Annealing [3] or Genetic Algorithms [4] to minimize trajectory and phase error. Optimization by shuffling magnets requires constructing a field error model from measurements of individual magnets, and then computing a "cost function" to be minimized. This may be done to good approximation for a pure-PM undulator by superposition of measured fields of individual magnets, since permeability of PM's is close to 1. In hybrid-PM undulators (HPMU'S) with ferromagnetic poles, linear superposition of PM fields is not valid. However, for small errors, "field error signatures" [5] can be obtained, which characterize the change in undulator field due to a small change in a magnetic or mechanical parameter, or of a magnetic shim [6]. Field error signatures may be scaled by Helmholtz data and convolved linearly with the ideal field, then integrated to compute trajectory and phase errors for a cost function to be minimized, by iterating thousands of times – a computationally intense process.

In this paper we extend the error signature concept and directly obtain trajectory kick, displacement and phase error signatures of magnetization errors. We show they are essentially decoupled and can then be simply scaled and summed to obtain a performance cost function. We outline a simple magnet swapping algorithm, written in Mathematica, to optimize spectral performance.

MAGNETIZATION ERROR SIGNATURES

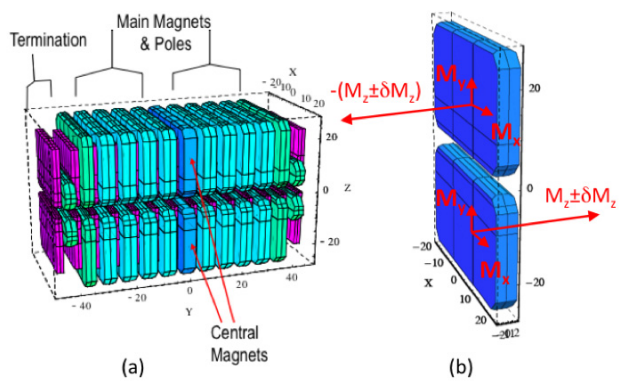

Figure 1. (a) Radia model of HPMU. (b) Central magnet pair with magnetization error components δM_z, M_y and M_x.

*This paper has been authored by employees of Brookhaven Science Associates, LLC, under Contract No. DE-AC02-98CH10886 with the US Department of Energy. The United States Government retains, and the publisher, by accepting the article for publication, acknowledges, a world-wide license to publish or reproduce the published form of this manuscript, or allow others to do so, for US Government purposes.

#rakowsky1@bnl.gov

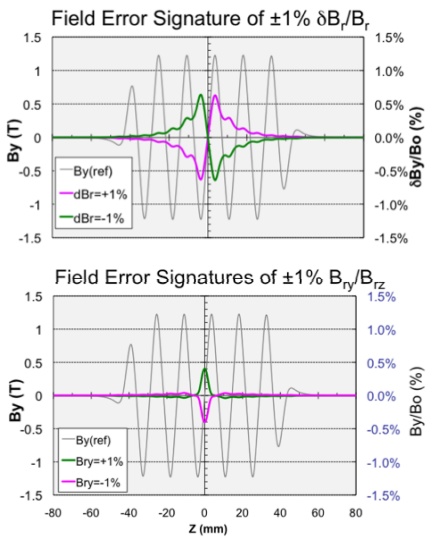

Figure 2(a). Field error signatures for ±1% errors in remanence (upper) and a ±1% y-component of magnetization (lower) in central magnet pair.

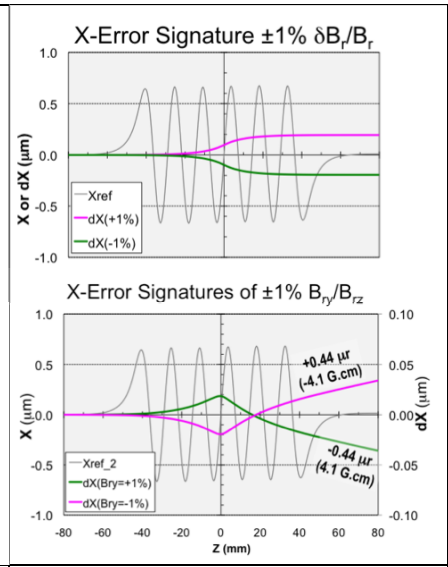

Figure 2(b). X-trajectory signatures for ±1% errors in remanence (upper) and ±1% y-magnetization component (lower) in central magnet pair.

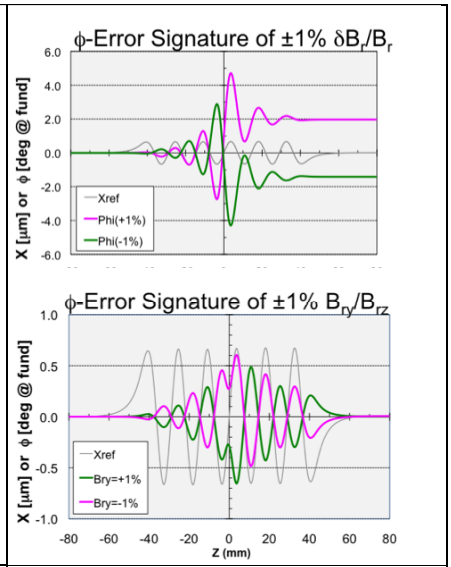

Figure 2(c). Phase error signatures for ±1% errors in remanence (upper) and ±1% y-magnetization (lower) in central magnet pair.

A short HPMU was modeled in Radia, with parameters of the NSLS X9 in-vacuum undulator: period λ_u=14.5 mm, 3.4 mm gap, NdFeB with B_r=1.3T. (Figure 1a.) On-axis fields $B_{y0}(z)$ and $B_{x0}(z)$ as well as trajectories $x_0(z)$ and $y_0(z)$ were computed with no errors applied. Nominal errors of ±1% in each component of magnetization were introduced in turn in the central magnet pair (Figure 1b): (a) $\delta M_z/M_z$ (the principal component) was simulated by changing B_r by ±1%; (b) M_y or M_x errors were modeled by adding ±0.01 transverse (x or y) components to the principal (z) magnetization unit vector. The transverse components were oriented to add on-axis. Again, on-axis fields and trajectories were computed for each case. Subtracting the no-error fields and trajectories, we obtain *field error signatures* and *trajectory error signatures* for each magnetization component. Finally, by computing the path length difference δS(z) between the trajectories with and without the error, normalized by the resonant optical wavelength, times 180°/π, we obtained phase error signatures (in degrees) for each error component.

Magnetization Strength Error

Figure 2 (upper row) shows the signatures of field error (%), X-trajectory error (μm) and phase error (degrees) due to ±1% error in B_r in the central magnet pair. Although the field error "bleeds" into 3 or 4 neighboring poles, it produces a net x-displacement of ~0.2 μm (~1/3 of the wiggle amplitude) with *no steering*. This gives us a scale factor of δx = ~0.1 μm per 1% δBr/Br per magnet. The phase error profile exhibits local over- and undershoots, but the *net* error is ~1.8 °, or δϕ = ~0.9°/ 1% δBr/Br per magnet.

Magnetization Angle Errors

Figure 2 (lower row) shows the signatures of a ±1% y-component of magnetization in both central magnets. The peak y-field error is ~0.3%, mostly localized at the magnet, and results in a net steering kick δx' of -/+0.44μr (~2 G.cm), or about -2 μr / 1% M_y/M_z per magnet. The phase error becomes oscillatory after the deflection, but the *average* phase shift is zero.

Not shown, a ±1% x-component of magnetization produces peak B_x field error of only 0.003%, a y-kick of 0.14μr, or 0.07 μr/1% M_x/M_z per magnet, and negligible phase error.

Performance Cost Function

These models reveal a simple scaling from Helmholtz or 3-axis far-field data of the magnet blocks:

- δM_z produces displacement δx and phase shift δϕ.
- M_y produces only an x-kick δx'.
- M_x produces only a y-kick δy'.

For small errors the scaling is linear. The models also reveal that the three magnetization error components produce effects that are essentially decoupled. For any arrangement of magnets we can now construct x and y error trajectories and phase error profiles by simple recursion. (The ± means that the appropriate sign must be applied depending on magnet location and orientation.)

- $x'_{i+1} = x'_i \pm \delta x'_{i+1}$; $x_{i+1} = x_i \pm \delta x_{i+1} + x'_{i+1}\,\lambda_u/2$
- $y'_{i+1} = y'_i \pm \delta y'_{i+1}$; $y_{i+1} = y_i + y'_{i+1}\,\lambda_u/2$
- $\phi_{i+1} = \phi_i + \delta\phi_{i+1}$ (independent of orientation)

The results are *net* error trajectories (minus local details), from which we can compute rms values, and combine them into a weighted multi-parameter cost function *W*:

$$W = a\,[h\,x_{rms}^2\,(\text{upper}) + h\,x_{rms}^2\,(\text{lower}) + x_{rms}^2\,(\text{both})] + b\,[h\,y_{rms}^2\,(\text{upper}) + h\,y_{rms}^2\,(\text{lower}) + y_{rms}^2\,(\text{both})] + c\,[h\,\phi_{rms}^2\,(\text{upper}) + h\,\phi_{rms}^2\,(\text{lower}) + \phi_{rms}^2\,(\text{both})],$$

where *a, b, c* are relative weights we assign to x, y and phase terms. We include cost terms for the upper and lower arrays individually (weighted by *h*) to avoid the case of large equal and opposite errors in the upper and lower arrays cancelling on-axis.

A MAGNET SORTING ALGORITHM

Figure 3 illustrates a simple magnet swapping routine. At each iteration two magnets are swapped at random, and assigned a random (odd or even) orientation. *W* is computed and the swap is accepted or rejected, based on Steepest Descent, Simulated Annealing or other rules. Since computation involves just simple running sums, the algorithm takes only minutes to test >10,000 swaps and reduce *W* to a small value (limited by data accuracy.) Many runs can be done to select the "best-of-the-best".

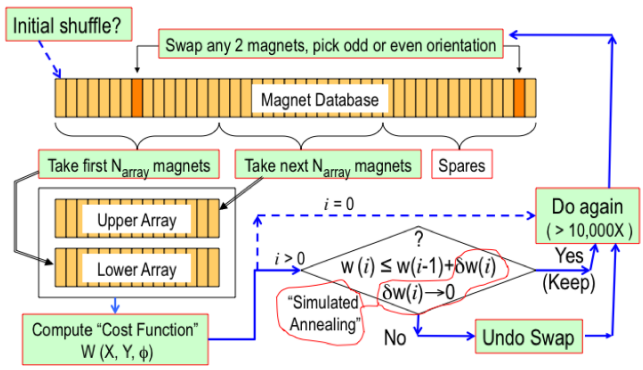

Figure 3. A simple magnet swapping algorithm.

Example

The optimization process described above was applied to the 23-period X9 IVU installed in 2008. (At the time the cost function only reflected trajectory error.) The magnet database consisted of 120 magnets. They were measured with a 3-axis Fluxgate Magnetometer in a fixture allowing accurate placement of magnets in each of 4 possible orientations. Sensor and fixture misalignment errors are cancelled by averaging. The magnet strength variation was within ±1%, while the angle error was 1.25±0.5°. The systematic error of 1.25° was in the y direction. The algorithm in Figure 4 was implemented in Mathematica. The code selected 45 magnets at random for each array. Some starting arrangements had X walk-offs up to twice the wiggle amplitude, and peak phase excursions up to 6°. After 10,000 iterations, whether by steepest descent or a simplified SA rule, the predicted peak X error reduced to <1/10 of a wiggle amplitude, with phase error <0.5°. Y trajectories, even random ones, were <1/10 of a wiggle amplitude. The X9 IVU, as built, achieved a trajectory that needed no shimming (except at the terminations) and a phase error of <2° rms. We plan to test the algorithm with phase error minimization included, on a longer IVU now under construction.

OTHER MAGNETIC SIGNATURES

Vertical pole displacement was modeled in a symmetric version of our Radia model. The field error is peaked at the pole, and produces a kick δx'=-0.044 μr and a phase step δϕ=~0.01° per μm of displacement. If pole heights in each array are first mapped on a coordinate measuring machine, it may be possible to compensate these fixed trajectory and phase errors by magnet shuffling as well.

Vertical magnet displacement has an anti-symmetric field error signature, which produces a non-steering displacement δx=~0.001 μm and a phase step δϕ=~0.005° per μm of displacement. Pole and magnet vertical displacements are frequently used for "virtual shimming".

We also modeled two types of inhomogeneity. (1) For a vertical gradient in M_z we found the poles effectively homogenize the variations. (2) A horizontal gradient in M_z, on the other hand, produces small, equal and opposite transverse gradients in field at adjacent poles, resulting in a small, non-steering, x-dependent x-displacement.

CONCLUSIONS

The magnet sorting described here lends itself to the "all-at-once" undulator assembly approach. For meaningful sorting, magnet measurements should resolve the variations in magnetization to at least 3 significant figures. Since magnets have tolerances of <1% and <1°, measurements should have resolution and *relative* accuracy to a part in 10^5 (10 ppm). This is a challenging requirement, limited mainly by instrument drift. Besides a magnetically and thermally stable environment, one needs to track the drift by frequently re-measuring a reference magnet while characterizing all the magnets. These precautions are being applied to our next undulator.

ACKNOWLEDGEMENT

Many thanks to T.Tanabe and O.Chubar for fruitful discussions, to J.B. Murphy and L-H Yu for Mathematica programming tips, and to J. Rank, D.A. Harder, M. Lehecka and T. Corwin for engineering and tech support.

REFERENCES

[1] O. Chubar, P. Elleaume, J. Chavanne, J.Synchrotron Rad. (1998) 5, 481-484
[2] Y. Li, B. Faatz, J. Pflueger, "Magnet Sorting for the XFEL Hybrid Undulator – Comparing Study", FEL 2007, Novosibirsk, Russia
[3] A.D. Cox, B.P. Youngman, Proc. SPIE 582 (1985) 91.
[4] O.Chubar, O.Rudenko et al., "Application of Genetic Algorithms to Sorting, Swapping and Shimming of the SOLEIL Undulator Magnets", SRI-2006, AIP Conf. Proc. vol.879, p.359 (2006).
[5] J.A. Clarke, D.J. Scott, "Hard X-ray Undulators in Intermediate Energy Light Sources", Proc. Shanghai Symposium on Intermediate-energy Light Sources, Sept. 24-26, 2001, Shanghai, China.
[6] B. Diviacco, R.P. Walker, Nucl. Inst. & Meth. A 368 (1996) 522-532.